J Fluoresc (2007) 17:223–234
DOI 10.1007/s10895-007-0161-9

ORIGINAL PAPER

Fluorescent Temporin B Derivative and its Binding to Liposomes

Rohit Sood · Yegor Domanov · Paavo K. J. Kinnunen

Received: 7 September 2006 / Accepted: 17 January 2007 / Published online: 6 February 2007

Abstract Temporins are short (10–13 amino acids) and linear antimicrobial peptides first isolated from the skin of the European red frog, *Rana temporaria*, and are effective against Gram-positive bacteria and *Candida albicans*. Similarly to other antimicrobial peptides, the association of temporins to lipid membranes has been concluded to underlie their antimicrobial effects. Accordingly, a detailed understanding of their interactions with phospholipids is needed. We conjugated a fluorophore (Texas Red) to a Cys containing derivative of temporin B (temB) and investigated its binding to liposomes by fluorescence spectroscopy. Circular dichroic spectra for the Cys-mutant recorded in the absence and in the presence of phospholipids were essentially similar to those for temB. A blue shift in the emission spectra and diminished quenching by ferrocyanide (FCN) of Texas Red labeled temporin B (TRC-temB) were seen in the presence of liposomes. Both of these changes can be attributed to the insertion of the Texas Red into the hydrophobic region of the bilayer. Resonance energy transfer, steady state anisotropy, and fluorescence lifetimes further demonstrate the interaction of TRC-temB with liposomes to be enhanced by negatively charged phospholipids. Instead, cholesterol attenuates the association of TRC-temB with membranes. The interactions between TRC-temB and liposomes of varying negative surface charge are driven by electrostatics as well as hydrophobicity. Similarly to native temporin B also TRC-temB forms amyloid type fibers in the presence of negatively charged liposomes. This property is likely to relate to the cytotoxic activity of this peptide.

Keywords Antimicrobial peptides · Texas Red · Liposomes · Hydrophobicity · Fluorescence spectroscopy

Abbreviations

AMPs	antimicrobial peptides
C-temB	cysteine temporin B
CHCA	α-cyano-4-hydroxycinnamic acid
Chol	cholesterol
CD	circular dichroism
EDTA	ethylenediaminetetraacetic acid
ET	energy transfer efficiencies
FRET	fluorescence resonance energy transfer
FCN	potassium ferrocyanide
HPLC	high pressure liquid chromatography
K_{SV}	Stern-Volmer quenching constant
k_q	bimolecular quenching constant
LUV	large unilamellar vesicles
NBD-PC	1-oleoyl-2-[6-[7-nitro-2-1,3-benzoxadiazol-4-yl)amino]hexanoyl]-sn-glycero-3-phosphocholine
POPG	1-palmitoyl-2-oleoyl-*sn*-glycero-3-phospho-rac-glycerol
PC	phosphatidylcholine
PG	phosphatidylglycerol
PIP_2	phosphatidylinositol-4,5-biphosphate
Q	quencher
RhB	rhodamine B
r	fluorescence anisotropy
SOPC	1-stearoyl-2-oleoyl-*sn*-glycero-3-phosphocholine
TRM	Texas Red maleimide
TRC-temB	Texas Red labeled temporin B

R. Sood · Y. Domanov · P. K. J. Kinnunen (✉)
Helsinki Biophysics and Biomembrane Group,
Medical Biochemistry,
Institute of Biomedicine,
University of Helsinki,
P.O. Box 63 (Haartmaninkatu 8),
Helsinki, FIN-00014 Finland
e-mail: Paavo.Kinnunen@Helsinki.Fi

TR	Texas Red
TFA	trifluoroacetic acid
λ_{max}	fluorescence emission maximum
τ	fluorescence lifetime

Introduction

Antimicrobial peptides (AMPs) constitute part of the non-adaptive host immunity providing a first line of defense against a wide spectrum of pathogens and are found in species ranging from protozoa to vertebrates [1, 2]. An increasing number of AMPs such as cecropins, defensins, magainins, temporins, melittin, indolicidin, plantaricin, nisin, and alamethicin, has been discovered in animals, plants, as well as bacteria. In mammals, these peptides are present on mucosal surfaces and skin, and are stored in the secretary granules of leukocytes, for instance. AMPs represent an active area of research aiming at the development of new antibiotics, anticancer drugs, food preservatives, and antiseptic agents [3].

One of the key properties of the AMPs is their ability to differentiate between foreign and host cells. Importantly, eukaryotic and bacterial membranes have very different lipid compositions. More specifically, the outer leaflet of the former cells comprises mainly of phosphatidylcholine, sphingomyelin, and cholesterol, whereas bacteria expose negatively charged phospholipids, phosphatidylglycerol, cardiolipin, and lipopolysaccharides [4]. Common features in most AMPs are their amphipathic character and net positive charge [5]. Accordingly, AMPs interact preferentially with acidic lipids [6, 7] which are thought to represent the molecular targets for these peptides [8, 9] and to provide in part a mechanistic basis for the differences in target cell specificity [10]. Under physiological conditions anionic phospholipids in mammalian cell plasma membranes are not exposed on their outer surface but retained in the cytoplasmic leaflet [11]. Along theses lines, the selectivity of some AMPs and cytotoxic proteins against cancer cells is likely to reflect the exposure of the negatively charged phosphatidylserine (PS) on the outer surface [12]. To this end, anionic phospholipids appear to play a rather general role in mediating the lipid binding of peptides and proteins and in their insertion and translocation across the lipid bilayer [13, 14]. In contrast, cholesterol has been shown to reduce the membrane binding of AMPs [15].

Ability to define the precise structure-function relationship for antimicrobial peptides would have important implications for the design of new therapeutic agents that could be used to counter bacterial infections and to combat the emerging of antibiotic resistant strains. The structures and amino acid compositions of natural AMPs have been modified to produce improved antibacterial and antifungal agents with high levels of antibiotic activity and low levels of hemolytic activity. This can be achieved for instance by altering their amino acid sequences to increase the net positive charge and hydrophobicity by lysine and tryptophan substitutions, respectively [16–18], conjugation of peptides with lipophilic moieties [19], incorporation of a carbamate bond [20], synthesis of hybrid peptides [21], and synthesis of truncated sequences without regions identified to be hemolytic [22]. Recently, Janmey and his coworkers [23] have shown that effective antimicrobial agents are obtained by conjugating rhodamine B (RhB) to peptides corresponding to the PIP_2-binding site of gelsolin. These short (mostly composed of ten amino acids) RhB labeled peptides possess antibacterial activity against Gram-negative and Gram-positive bacteria, while the nonlabeled peptides and gelsolin as such are ineffective. It was proposed that the coupling of RhB to the peptide increases its net hydrophobicity and thus increases its membrane permeation [23].

Behaviour of various AMPs has been characterized in detail in the presence of model membranes. AMPs typically show several characteristics in the presence of lipid membranes such as a change in the conformation from a random coil to alpha helical, further augmented in the presence of negatively charged phospholipids [24]. It has been shown that various amphipathic α-helical peptides such as magainin, cecropin B, cecropin P, dermaseptin B, and dermaseptin S bind to and permeate zwitterionic membranes, although 10-fold higher concentrations are needed compared with negatively charged membranes [25, 26]. Recently, we have compared the effects of the AMPs like temporin B, temporin L, indolicidin, magainin 2, and plantaricin A on the zwitterionic as well as negatively charged membranes [6, 15, 27]. In brief, magainin 2, temporin B and plantaricin A have pronounced effects on the membranes containing negatively charged phospholipids while only a minor impact on zwitterionic membranes was evident. Temporin L and indolicidin preferentially bind to acidic phospholipids, yet they also exhibit significant interactions with zwitterionic membranes. Fluorescence studies of these peptides in lipid bilayers in the presence of pyrene labeled lipids have shown that they increase the acyl chain order in the presence of POPG, the magnitude of this effect increasing with the content of this lipid [15]. Likewise, lipid segregation was induced by these peptides in the presence of the acidic phospholipid. All these effects again emphasize the importance of acidic phospholipids as well as the cationic charges of the peptides for their interaction with target membranes. Interestingly, following the binding of AMPs to their lipid targets they somehow disrupt the barrier properties of the membranes [28–32]. AMPs have been reported to form amyloid like fibers in the presence of acidic phospholipids [27].

Amyloid fibers are ordered aggregates of peptides or proteins that are fibrillar in structure and contribute to the

complications of many diseases for example, type 2 diabetes mellitus, Alzheimer's disease, and primary systemic amyloidosis. These fibers have a cross-β-sheet structure in which polypeptide chains are oriented in such a way that the β-strands run perpendicularly to the long axis of the fibril, while β sheets propagate in its direction. The physicochemical basis of amyloid formation remains incompletely understood. There seems to be a consensus about peptide aggregation being prompted by partial unfolding of proteins [33, 34]. This can be consistently enhanced in a slightly hydrophobic environment at acidic pH and both hydrophobicity and the net charge of the protein seem to be crucial, neutralization of the charges triggering aggregation. These conditions are readily found in membranes containing acidic phospholipids and it has indeed been demonstrated recently, that such membranes trigger the growth amyloid fibrils by a range of cationic proteins and peptides [12, 27, 35]. The membranes additionally provide a highly anisotropic environment, efficiently aligning the peptides in the lipid–water interface [36]. This process appears to be driven by coulombic forces between the cationic residues of the proteins and the acidic phospholipids, exhibiting no specificity to the latter. Finally, we have concluded it to be highly likely that AMPs permeabilize their target membranes by the same mechanism as amyloid protofibrils in general [27].

Among the smallest AMPs identified to date are those isolated from amphibian skin [48]. In this respect temporins, a family of cationic, 10–13 residue peptides isolated from *Rana temporaria*, the red frog found in Central Europe [37], are of particular interest. Thought at first to be exclusive to *R. temporaria*, novel members of the temporin family have recently been isolated also from other species of the genus *Rana*, [38] viz., *R. clamitans* [39], *luteiventris* [38], *pipiens* [38], and *grylio* [40]. Temporins are particularly active against gram-positive bacteria and *Candida albicans*, yet generally non-toxic (non-hemolytic) to human red blood cells [41, 42]. In order to facilitate the assessment of the properties of these peptides by fluorescence spectroscopy we conjugated by nucleophilic addition to CLLPIVGNLLKSLL-COOH (C-temB i.e. temporin B bearing an additional cysteine residue at the *N*-terminus) a maleimide derivative of the stable, high quantum yield fluorophore, Texas Red (TR). Prolonged fluorescence lifetimes of TRC-temB in buffer compared to free TR reflect an increased hydrophobicity in the environment of the fluorophore in the labeled peptide.

Liposomes were used as model membranes and were composed of 1-stearoyl-2-oleoyl-*sn*-glycero-3-phosphocoline (SOPC), 1-palmitoyl-2-oleoyl-*sn*-glycero-3-phospho-rac-glycerol (POPG), and β-cholesterol, as indicated. CD measurements revealed a change in the conformation of C-temB from random coil in buffer to an α-helix in the presence of liposomes, with the extent of helicity increasing further in the presence of negatively charged phospholipids. Subsequently, we wanted to study which fluorescence spectroscopy features could be utilized to distinguish between lipid-dependent changes in (i) the extent of membrane binding, (ii) in the mode of membrane association, and (iii) peptide aggregation and oligomer formation. Binding of TRC-temB to membranes was demonstrated by resonance energy transfer (FRET) between TR and the fluorescent 1-oleoyl-2-[6-[7-nitro-2-1,3-benzoxadiazol-4-yl)amino]hexanoyl]-sn-glycero-3-phosphocholine (NBD-PC) lipid incorporated into liposomes. Efficiency of energy transfer was enhanced in the presence of negatively charged phospholipids while cholesterol attenuated FRET. The binding of TRC-temB to lipid membranes induced a blue shift in TR emission. Presence of cholesterol in the liposomes attenuated the binding of the peptide as reflected by the negligible shift in the emission maxima, smaller steady state anisotropy, and prolonged fluorescence lifetimes of the fluorophore. These results were further supported by steady state and time resolved fluorescence quenching studies, which showed that TRC-temB inserts into the hydrophobic region of the bilayer. TRC-temB formed amyloid-like fibers in the presence of negatively charged liposomes. Our data indicate TRC-temB to be a highly environment sensitive fluorescent peptide analog for assessing lipid interactions.

Experimental procedures

Materials and methods

Hepes, EDTA, Congo red, and α-cyano-4-hydroxycinnamic acid (CHCA) were from Sigma. HPLC grade trifluoroacetic acid (TFA) was from Fluka (Buchs, Switzerland), potassium ferrocyanide from Merck, and acetonitrile from Rathburn (Walker Burn, Scotland, UK). SOPC[1], POPG, and β-cholesterol were from Avanti Polar Lipids (Alabaster, AL). NBD-PC and Texas Red maleimide (TRM) were from Molecular Probes (Eugene, OR). The purity of lipids was checked by thin-layer chromatography on silicic acid coated plates (Merck, Darmstadt, Germany) developed with a chloroform/methanol/water mixture (65:25:4, v/v/v). Examination of the plates after iodine staining and when appropriate upon UV illumination revealed no impurities. Concentrations of the nonlabeled lipids were determined gravimetrically with a high precision electrobalance (Cahn, Cerritos, CA). Concentration of the fluorescent lipid analogue NBD-PC was determined spectrophotometrically using a molar absorptivity $\varepsilon_{465} = 19000\ \mathrm{M^{-1}cm^{-1}}$ (in C_2H_5OH). The indicated temporin B derivative was synthesized by Synpep (Dublin, CA) and its purity ($> 98\%$) was verified by HPLC and mass spectrometry. All experiments were conducted in

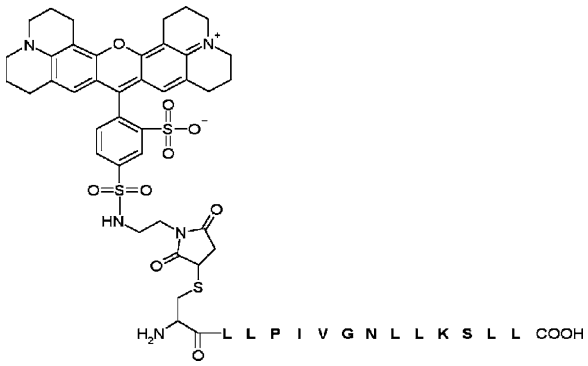

Fig. 1 Schematic representation of chemical structure of Texas Red labeled Cys-temporin B (TRC-temB). Please note that the structure of the fluorophore and the peptide sequence have not been drawn to be on the same scale

5 mM Hepes, 0.1 mM EDTA, pH 7.0 unless otherwise indicated.

Coupling of Texas Red to C-temB

To avoid aggregation and precipitation of TRM and the peptide during conjugation, the reaction was carried out in 20 mM Hepes, 0.1 mM EDTA, pH 7.0 containing 20% (by volume) acetonitrile. TRM and C-temB were mixed in 1:1 molar ratio at a final concentration of 50 μM and this mixture incubated for 3 h in the dark with stirring. Labeled peptide (TRC-temB) was then purified by HPLC on a reverse phase column (μRPC C2/C18 ST 4.6/100, Amersham Biosciences, Uppsala, Sweden) eluted with a linear gradient from 20 to 80% acetonitrile in water with 0.05% TFA. No unreacted label was detected by chromatography and no unlabeled peptide was detected by mass spectrometry thus indicating that the peptide was completely labelled. The mass of the fluorescent peptide derivative (Fig. 1) was confirmed by mass spectrometry on flex Control MALDI-TOF (Bruker Daltonics, Bremen, Germany) and with a saturated solution of CHCA in 33% acetonitrile, 0.1% TFA as matrix.

Preparation of large unilamellar vesicles (LUVs)

Appropriate amounts of the lipid stock solutions were mixed in chloroform to obtain the desired compositions. The solvent was removed under a stream of nitrogen, and the lipid residue was subsequently maintained under reduced pressure for at least 2 h. The dry lipids were then hydrated at room temperature for one hour in 5 mM Hepes and 0.1 mM ethylenediaminetetraacetic acid (EDTA, pH 7.0). The resulting dispersions were extruded through a single polycarbonate filter (pore size of 100 nm, Millipore, Bedford, MA) using a Lipofast low-pressure homogenizer (Avestin, Ottawa, ON) to produce LUVs, with an average diameter between 111 and 117 nm [43].

Measurement of circular dichroic (CD) spectra

UV-CD spectra from 250 to 190 nm were recorded with a CD spectrophotometer (Olis RSF 1000F, On-line Instrument Systems Inc., Bogart, GA) with the temperature maintained at 20°C with a circulating water bath. A 1-mm path length quartz cell was used at a final concentration of 50 μM and 3 mM of peptide and liposomes, respectively, in buffer. Interference by circular differential scattering by liposomes was eliminated by subtracting CD spectra for liposomes from those recorded in the presence of peptide. Data are shown as mean residue molar ellipticity (degrees cm^2 dmol^{-1}) and represent the averages of seven scans. The percentage of helical content was estimated from the molar ellipticity at 222 nm (θ_{222}) using the equation:

$$f_h = (\theta_{222}/\theta_{h222\alpha}) + (ik/N) \quad (1)$$

where f_h is the fraction in α-helical form, $\theta_{\mathrm{h}222\alpha}$ is the molar ellipticity at 222 nm for an infinitely long α-helix ($-39{,}5000$ deg cm^2/dmol), i is the number of helices (assumed to be one), k is a wavelength specific constant (2.6 at 222 nm), and N is the number of residues in the peptide [44].

Microscopy

Amyloid-type fiber formation was assessed by adding TRC-temB to a solution of SOPC/POPG LUVs (8:2 molar ratios) to yield final concentrations of 0.1–1.0 μM and 10 μM, respectively, in buffer. The samples were observed by bright field microscopy (Olympus IX 70, Olympus Optical Co., Tokyo, Japan). For polarized microscopy, the specimens were incubated for 30 min with 10 μM Congo red and their resulting birefringence was observed using crossed polarizers in the excitation and emission paths and birefringence images were taken with Canon colour camera.

When indicated, trace amounts ($X = 0.02$) of the fluorescent lipid NBD-PC was additionally included in to the liposomes, and fibers were formed as described above, imaging their fluorescence with an inverted microscope (Zeiss IM-35, Oberkochen, Germany) using mercury arc lamp as an excitation source. Filter sets appropriate for the observation of NBD (BP 450-490, FT 510, LP 520) and Texas Red (BP 546/12, FT 580, LP 590) were used. Images were acquired with a B/W CCD camera (C4742-95-12 NRB, Hamamatsu Photonics K. K., Hamamatsu, Japan) interfaced with a computer, and operated by the software (AquaCosmos) provided by the camera manufacturer.

Steady state fluorescence spectroscopy

Fluorescence measurements were carried out with a Perkin Elmer LS50B (Wellesley, MA) or a Cary Eclipse (Varian

Instruments, Walnut Creek, CA) spectrofluorometer interfaced to a computer. Cuvette temperature was maintained at 20°C with a circulating water bath, and the contents were agitated by a magnetic stirring bar. LUVs were added to a solution of TRC-temB (0.3 μM final concentration) in 5 mM Hepes, 0.1 mM EDTA, pH 7.0, in a total volume of 1 ml. After equilibration fluorescence spectra were recorded with both emission and excitation bandpasses set at 5 nm. Due to the very low concentrations of the chromophores used inner filter effect can be expected to be negligible. Texas Red was excited at 550 nm and emission spectra were recorded between 570 and 700 nm, averaging three scans. Spectra were corrected for the contribution of light scattering in the presence of vesicles. Although referred to as emission maxima (λ_{max}) throughout this communication, spectral center of mass instead of intensity maxima was employed to minimize the error in the determination of spectral shifts. S.D. for the given values of λ_{max} were less than 0.2 nm.

For the measurement of resonance energy transfer NBD-PC ($X = 0.01$) was included in the liposomes as a donor, and its fluorescence was monitored with excitation at 470 nm and emission at 530 nm, using 5 nm bandwidths, while varying the concentration of TRC-temB. The total concentration of phospholipids was 20 μM with temperature maintained at 20°C. Energy transfer efficiencies were calculated using the equation

$$E = (1 - F/F_0) \tag{2}$$

where F_0 and F represent the fluorescence intensities in the absence and the presence of the acceptor respectively.

Polarized emission was measured in the L-format using Polaroid film type filters with Perkin Elmer LS50B. Fluorescence anisotropy r of TR was measured with excitation at 550 nm and emission at 610 nm, using 10 nm bandwidths and was calculated using routines of the software provided by Perkin-Elmer.

Aliquots of concentrated solution of potassium ferrocyanide (FCN) were added to the peptide solution in the absence as well as in the presence of liposomes. The data were analyzed by the Stern-Volmer equation [45]:

$$F_0/F = 1 + K_{sv}[Q] = 1 + k_q\tau_0[Q] \tag{3}$$

where F_0 and F represent the fluorescence intensities in the absence and the presence of the quencher (Q), respectively, and K_{sv} is the Stern Volmer quenching constant, which is the measure of the accessibility of TR to FCN, and is defined as

$$K_{sv} = k_q\tau_0$$

where k_q is the bimolecular quenching constant and τ_0 is the lifetime of the fluorophore in the absence of the quencher.

Time resolved fluorescence measurements

Commercial laserspectrometer (Photon Technology International, Ontario, Canada) was used to measure fluorescence lifetimes. A train of 500 ps excitation pulses at 590 nm at a repetition rate of 10 Hz was produced by a nitrogen laser, pumping a dye laser (rhodamine 6G, Merck, Darmstadt, Germany, 6 mM solution in methanol). For the determination of the fluorescence lifetimes, the averages of the five emission decay curves were analyzed and were fitted as:

$$F(t) = \alpha\ \exp(-t/\tau) \tag{4}$$

where α_1 is a preexponential factor and τ_1 is the fluorescence lifetime of Texas Red. The decay parameters were recovered using a nonlinear least squares iterative fitting procedure based on the Marquardt algorithm [46]. The validity of the fit of a given set of observed data and chosen function was evaluated by the reduced chi 2 ($\chi_R{}^2$) values, the weighted residuals [47], and the autocorrelation function of the weighted residuals [48]. A fit was considered acceptable when plots of the weighted residuals and the autocorrelation function showed random deviation about zero with a minimum in $\chi_R{}^2$ value not exceeding 1.5. Instrument response function was measured separately using an aqueous glycogen solution. The minimum lifetime accessible to the instrument is 200 ps.

Results

CD spectroscopy

Several studies have demonstrated pronounced changes in the secondary structure of most AMPs upon their interaction with target phospholipids [49]. In an aqueous solution C-temB adopts a random coil structure, characterized by a single minimum in the CD spectra at 197 nm (Fig. 2). In the presence of SOPC LUVs, the peptide is α-helical with the characteristic double minima at 208 nm and 222 nm. Compared with the zwitterionic SOPC LUVs, the calculated helical content increases slightly, from 36 to 38% in the presence of SOPC/POPG (6:4, molar ratio) liposomes. Accordingly, the addition of cysteine and carboxylation of the C-terminus of the peptide did not alter the lipid-induced changes in the secondary structure of temB characteristic for AMPs.

Formation of amyloid like fibers

We have recently observed the ability of acidic phospholipid containing liposomes to induce a rapid formation of amyloid-type fibers *in vitro* by a variety of proteins such as lysozyme, insulin, glyceraldehyde-3-phosphate-dehydrogenase,

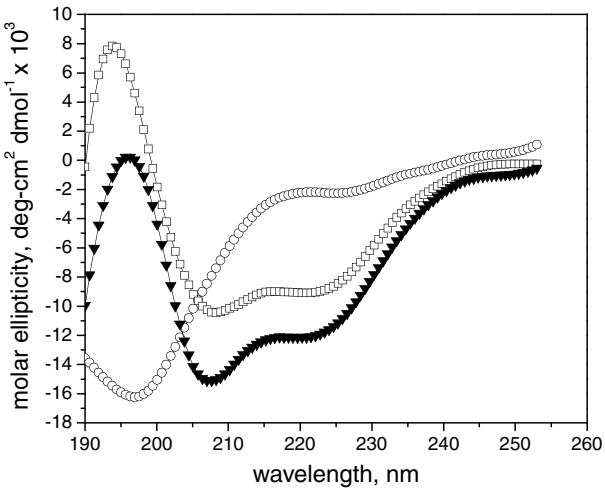

Fig. 2 Circular dichroic spectra of 50 μM C-temB in given buffer composition (○) and in the presence of LUVs composed of SOPC with $X_{POPG} = 0$ (□) and 0.4 (▼). Final lipid concentration is 3 mM. The temperature was maintained at 20°C with a circulating water bath

myoglobin, transthyretin, cytochrome c, histone H1, and α–lactalbumin and by several AMPs eg., temporin L, magainin, indolicidin and plantaricin A (for brief accounts see Refs. [27, 35]). Interestingly, all the above proteins and peptides have been shown to be involved in the triggering of apoptosis or killing of cancer cells. Along these lines, it was of interest to study if also TRC-temB could form amyloid-like fibers. Interestingly, we observed TRC-temB to form microscopic fibers in the presence of PG containing liposomes (Fig. 3A), with Congo red staining producing the characteristic light green birefringence (Fig. 3B). In addition to TR fluorescence (Fig. 3D) these fibers also showed intense NBD (Fig. 3C) fluorescence, when the fluorescent phospholipid analog NBD-PC was present in the liposomes. No fibers were seen in the presence of liposomes composed of PC only.

Steady state anisotropy studies

Rotational diffusion of fluorophores is the dominant cause of fluorescence depolarization. For proteins and peptides the mobility of the fluorescent moiety bears a close relationship with the overall state of biopolymers and factors that affect their size, shape, or segmental flexibility will also influence the observed values for the steady state anisotropy, r [50]. Accordingly, measurement of r provides a sensitive technique to study the association of any fluorescent molecule with membranes. Binding of TRC-temB to liposomes was first evaluated by recording r in the presence of increasing concentration of liposomes (Fig. 4). Values for r in the presence of SOPC/POPG (8:2 and 6:4 molar ratios) vesicles are higher than for neat SOPC vesicles whereas in the presence of SOPC/Chol (9:1 molar ratio) r is significantly reduced. These differences in r are likely to reflect difference in the extent of binding of TRC-temB to the above lipids.

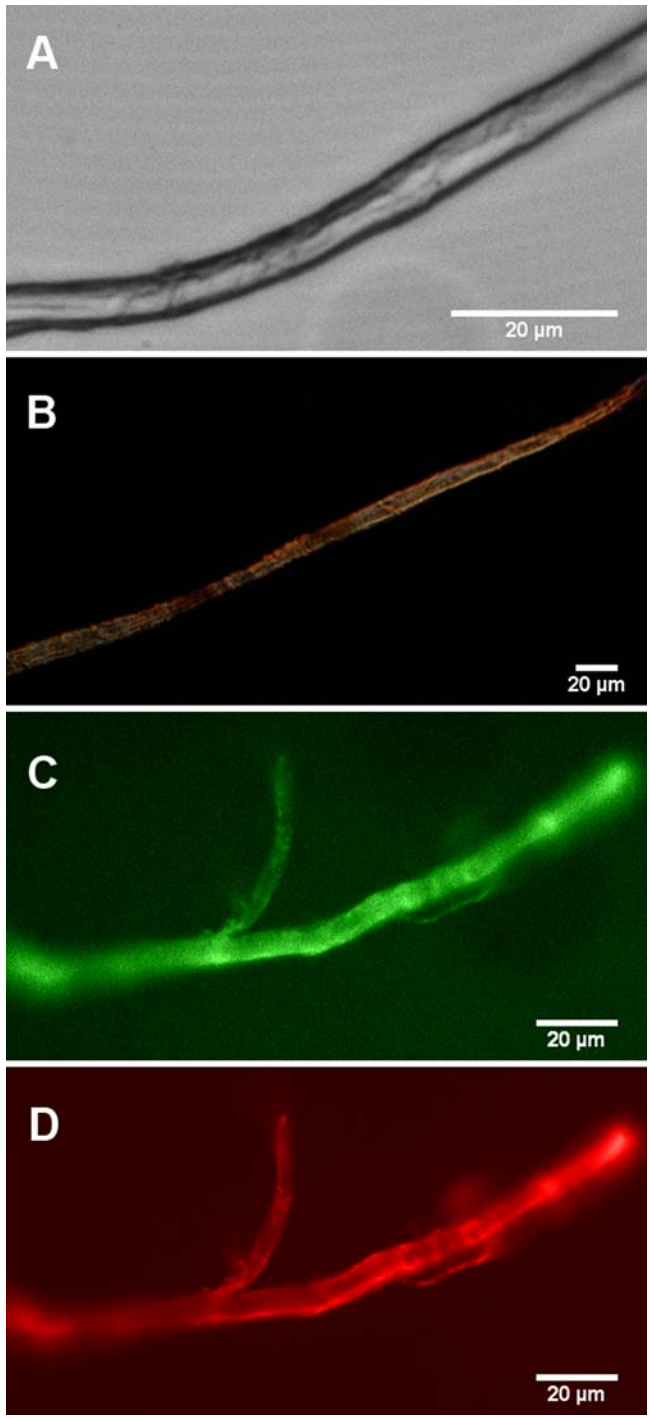

Fig. 3 *Panel A*. Bright field microscopy image of a fiber formed by TRC-temB after mixing with SOPC/POPG (8:2 molar ratio) liposomes at ambient temperature. The final concentrations of the phospholipid and peptide were 10 μM and 0.1–1.0 μM (approximately 24°C). Magnification was 40 × . *Panel B*: The fiber formed as shown in panel A but after staining with Congo red (final concentration of 10 μM). Magnification was 20 × . *Panel C*: Incorporation of the fluorescent phospholipid analogue NBD-PC into the fiber. The latter was formed as described above except that a trace amount ($X = 0.02$) of NBD-PC was additionally included in the SOPC/POPG liposomes. Magnification was 16 × . *Panel D*: The same fiber as shown in panel C but showing intense Texas Red fluorescence. Magnification was 16 ×

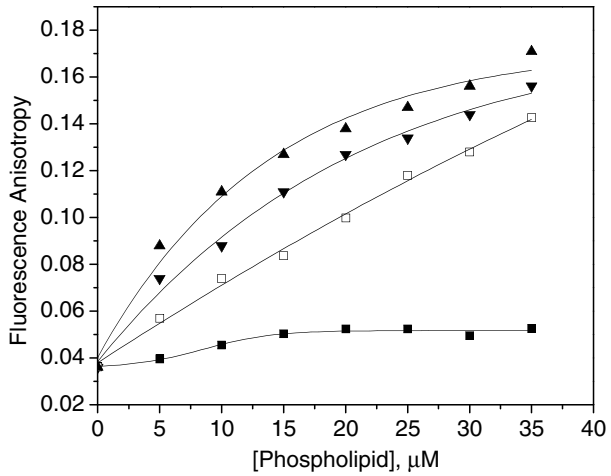

Fig. 4 Steady state fluorescence anisotropy *r* for liposomes composed of SOPC with $X_{POPG} = 0$ (□), 0.2 (▲), and 0.4 (▼) and with $X_{Chol} = 0.1$ (■) as a function of [phospholipid]. Each data point shown represents the mean of five measurements. Concentration of TRC-temB was 0.3 μM

Resonance energy transfer measurements

Lipid binding of TRC-temB was verified employing resonance energy transfer (RET) from NBD-labeled lipid (NBD-PC) incorporated into liposomes to TRC-temB. The two fluorophores, NBD and TR constitute a highly effective donor-acceptor pair and RET is demonstrated by the emission spectra recorded in the range of 450 to 650 nm for TRC-temB in the presence of SOPC/POPG/NBD-PC (79:20:1 molar ratios) liposomes (Fig. 5A). In an aqueous buffer the emission maximum for NBD-PC containing liposomes is observed at 535 nm. With increasing [TRC-temB] the intensity of NBD fluorescence decreases while emission of TR is progressively enhanced (Fig. 5A). In the presence of neat SOPC vesicles RET efficiency was low. The calculated energy transfer efficiencies (ET) were enhanced for SOPC/POPG vesicles, in keeping with augmented membrane binding or deeper penetration of TRC-temB into the bilayer in the presence of the negatively charged lipid (Fig. 5B). Electrostatic interaction is revealed by the partial reversal of RET upon the addition of NaCl after the completion of the membrane association of the peptide (Fig. 5A).

Steady state fluorescence quenching of TRC-temB by FCN

To gain further insight into the impact of lipid composition on the peptide/liposome interaction and to investigate the localization of TRC-temB in membranes we utilized collisional quenching of TR fluorescence by FCN. Addition of FCN decreases the fluorescence of TRC-temB both in the absence and in the presence of liposomes, without other effects on the recorded spectra (Fig. 6). However, quenching becomes

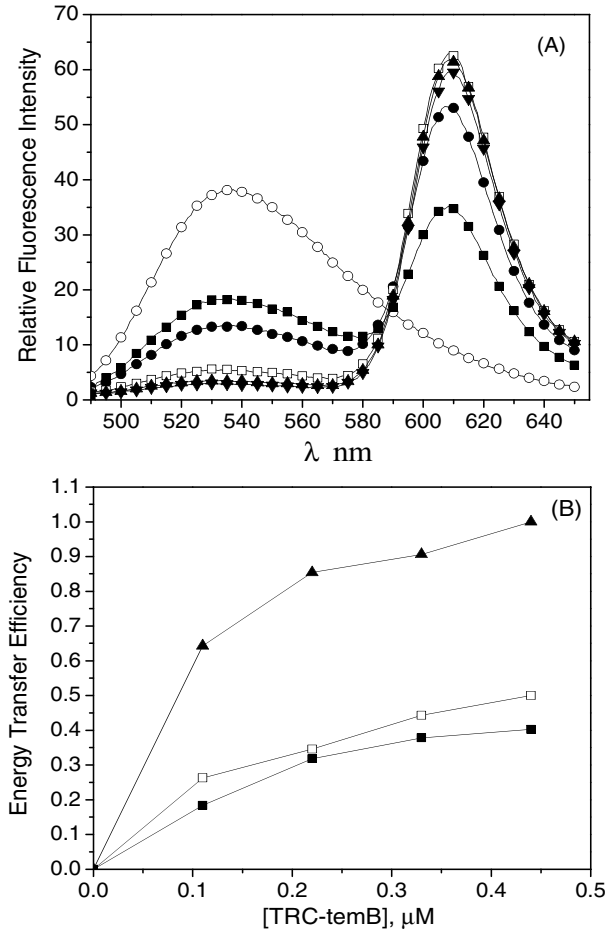

Fig. 5 *Panel A*: Emission spectra for NBD-PC ($X = 0.02$) containing SOPC/POPG (8:2 molar ratio) liposomes in the buffer (○) and in the presence of 0.1 (●), 0.2 (□), 0.3 (▲), and 0.4 μM (▼) of TRC-temB and 260 mM NaCl (■) added to 0.4 μM of TRC-temB. The excitation was at 470 nm. *Panel B*: Efficiency of energy transfer from NBD to TRC-temB as function of peptide concentration in the presence of liposomes composed of SOPC (□), SOPC with $X_{POPG} = 0.2$ (▲), and SOPC with $X_{Chol} = 0.1$ (■)

less efficient in the presence of liposomes thus demonstrating the fluorophore to be accommodated within the bilayer, as reflected in the Stern-Volmer quenching constant K_{sv} (Table 1). More specifically, K_{sv} decreases in the presence of both SOPC and SOPC/POPG LUVs, revealing reduced access of the quencher to the fluorophore. Comparison of K_{sv} and k_q values for POPG containing and neat SOPC liposomes further show that the binding of TRC-temB to liposomes is enhanced in the presence of POPG. Accordingly, both K_{sv} and k_q decrease as X_{POPG} is increased from 0.0 to 0.4. In contrast, the values for K_{sv} measured with cholesterol containing liposomes are slightly higher than for SOPC. These data suggest the affinity of TRC-temB for liposomes and/or the depth of the membrane penetration of TR to increase in the order SOPC/Chol (9:1) < SOPC < SOPC/POPG (9:1) < SOPC/POPG (8:2) < SOPC/POPG (6:4).

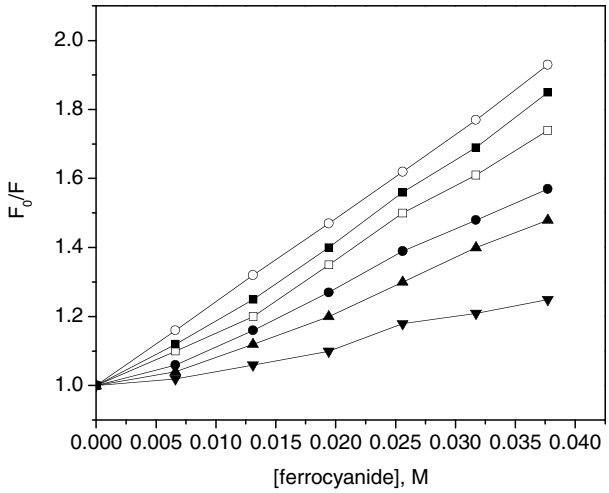

Fig. 6 Stern-Volmer plots for the quenching of TRC-temB fluorescence by FCN in the aqueous buffer (○) and in the presence of liposomes composed of SOPC (□), SOPC/POPG with $X_{POPG} = 0.1$ (●), 0.2 (▲), and 0.4 (▼) and SOPC/Chol with $X_{Chol} = 0.1$ (■)

Time resolved fluorescence spectroscopy

Not only the spectral features but also the fluorescence lifetimes (τ) of a fluorophore depend on its microenvironment [50]. A representative emission decay curve is illustrated (Fig. 7A) and the values of τ, and reduced chi squared (χ_R^2) obtained from these decays for TRC-temB in buffer as well as in the presence of liposomes are compiled in Table 2. The values for χ_R^2 reveal a good fit with the calculated mono-exponential decays. In buffer τ was 5.2 ns, which is slightly longer than the reported value for the free Texas Red fluorophore in an aqueous solution, 4.2 ns [50]. The τ values of TR are prolonged further in the presence of liposomes with a maximum of 6.0 ns detected for SOPC liposomes. We also measured time-resolved quenching of TRC-temB TR by FCN in the absence as well as in the presence of liposomes, with τ_0 and τ representing the fluorescence lifetimes for TR in the absence and in the presence of FCN, respectively (Fig. 7B). Stern-Volmer quenching constants K_{sv}^{TF} calculated from these data are shown in Table 1 and are in perfect agreement with the values for K_{sv} derived from the steady state measurements.

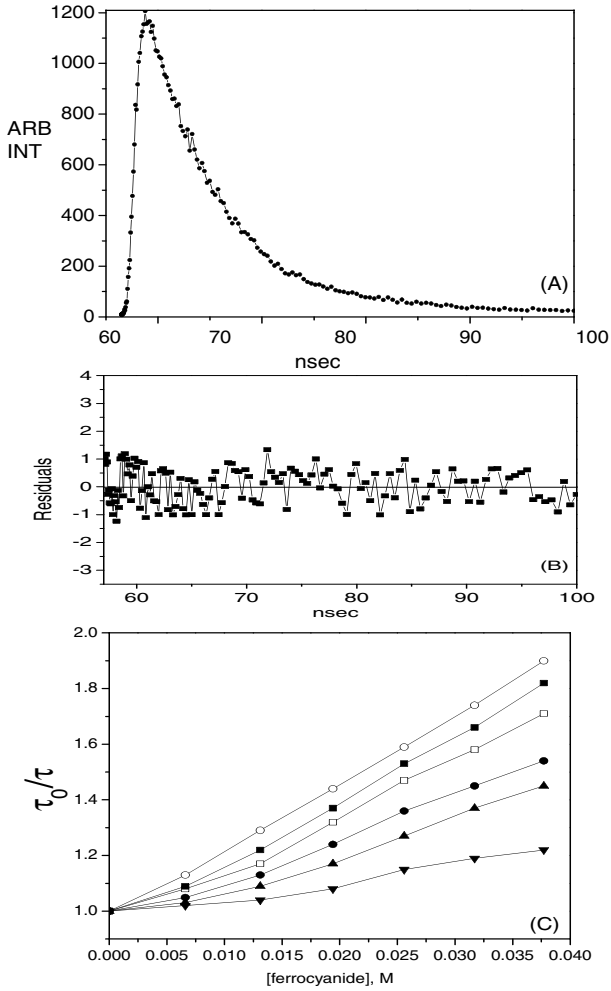

Fig. 7 *Panel A*: Time resolved fluorescence intensity decay for TRC-temB in buffer (●) at 20°C. The [phospholipid] in these set of experiments was 20 μM. *Panel B:* shows the weighted residuals. The excitation wavelength was 590 nm and emission wavelength was monitored at 610 nm. *Panel C*: Stern-Volmer plots for the quenching of time resolved TRC-temB fluorescence of FCN in aqueous buffer (○) and in the presence of liposomes composed of SOPC with $X_{POPG} = 0$ (□), 0.1 (●), 0.2 (▲), and 0.4 (▼), and SOPC/Chol with $X_{Chol} = 0.1$ (■)

Table 1 The Stern-Volmer quenching constant K_{sv} (steady state fluorescence), K_{sv}^{TR} (time resolved fluorescence) (M^{-1}) and bimolecular quenching constant ($k_q \times 10^{-9}$ M^{-1} s^{-1}) of FCN for TRC-temB in the absence as well as in the presence of liposomes

Liposomes	K_{sv}	k_q	K_{sv}^{TR}
Buffer	24.50 ± 0.16	4.71	24.00 ± 0.37
SOPC/Chol			
$X_{Chol} = 0.1$	22.73 ± 0.57	3.72	22.21 ± 0.83
SOPC	20.12 ± 0.67	3.35	19.48 ± 0.90
SOPC/POPG			
$X_{POPG} = 0.1$	15.80 ± 0.56	2.68	15.06 ± 0.74
$X_{POPG} = 0.2$	13.29 ± 0.70	2.37	12.53 ± 0.91
$X_{POPG} = 0.4$	7.10 ± 0.48	1.37	6.30 ± 0.54

Table 2 Fluorescence lifetimes (τ, ns), and χ_R^2 values for TRC-temB obtained from the single exponential decays recorded in the absence and in the presence of SOPC/POPG liposomes with the indicated mole fraction of the anionic phospholipid

		X_{POPG}			
TRC-temB in buffer		0.0	0.1	0.2	0.4
τ	5.2	6.0	5.9	5.6	5.8
χ_R^2	1.1	1.3	1.2	1.2	1.1

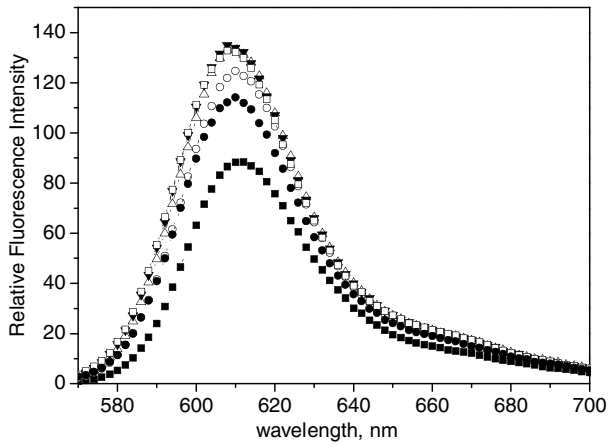

Fig. 8 Fluorescence spectra of TRC-temB in an aqueous buffer (■) and in the presence of increasing concentration of liposomes composed of SOPC with POPG (6:4). [TRC-temB] was 0.3 μM with total [Phospholipid] increasing as 20 (○), 40 (△), 60 (▼), and 80 μM (□). (●) represents the effect of NaCl (260 mM) added after the peptide titration. The temperature was maintained at 20°C with a circulating water bath

Binding of TRC-temB to liposomes

The changes in fluorescence emission characteristics of TR upon binding of TRC-temB to membranes is demonstrated by the impact of increasing concentrations of SOPC/POPG (6:4 molar ratio) liposomes (Fig. 8). In keeping with the association of TRC-temB with lipid bilayers, the λ_{max} in buffer at 617 nm shifts to shorter wavelengths in the presence of liposomes (Fig. 9A), together with an increase in the relative fluorescence intensity (Fig. 8). The above changes in emission indicate decreased polarity of the solvent environment of TR. Compared to zwitterionic liposomes the change in $\Delta\lambda_{max}$ was more pronounced in the presence of liposomes containing negatively charged phopholipids (Fig. 9A). Interestingly, $\Delta\lambda_{max}$ in the presence of liposomes devoid of negatively charged lipid was much smaller than for SOPC/POPG samples, indicating reduced binding of the peptide to zwitterionic membranes (9:1, Fig. 9A). Addition of NaCl (260 mM) after titration with the peptide partially reverses the above changes in λ_{max} thus emphasizing also coulombic attraction to be involved in the binding of TRC-temB to membranes (Table 3). Association of TRC-temB with SOPC vesicles causes only minor changes in the fluorescence intensity. However, in the presence of POPG, a pronounced and progressive enhancement in intensity becomes evident (Fig. 9B), while in the presence of cholesterol fluorescence intensity decreases. Smallest shift in the emission maxima of TR and decrease in fluorescence intensity is evident for liposomes containing cholesterol, thus suggesting that cholesterol either attenuates the membrane association of TRC-temB or that in the presence of this lipid the peptide resides in the surface of the bilayer. These two possibilities are not mutually exclusive. The affinity of the peptide increasing in the sequence SOPC/Chol (9:1) ∼ SOPC < SOPC/POPG (9:1) < SOPC/POPG (6:4) < SOPC/POPG (8:2).

Table 3 Values of λ_{max} for TRC-temB in the presence of liposomes and after the addition of NaCl

[Liposomes, μM]	80 μM	[NaCl] = 260 mM
SOPC	616.1	616.9
SOPC/Chol		
X_{Chol} = 0.1	616.6	616.9
SOPC/POPG		
X_{POPG} = 0.1	613.4	615.0
X_{POPG} = 0.2	614.7	615.8
X_{POPG} = 0.4	613.8	614.9

Discussion

We assessed the membrane binding of TRC-temB by monitoring changes in the fluorescence of the covalently coupled

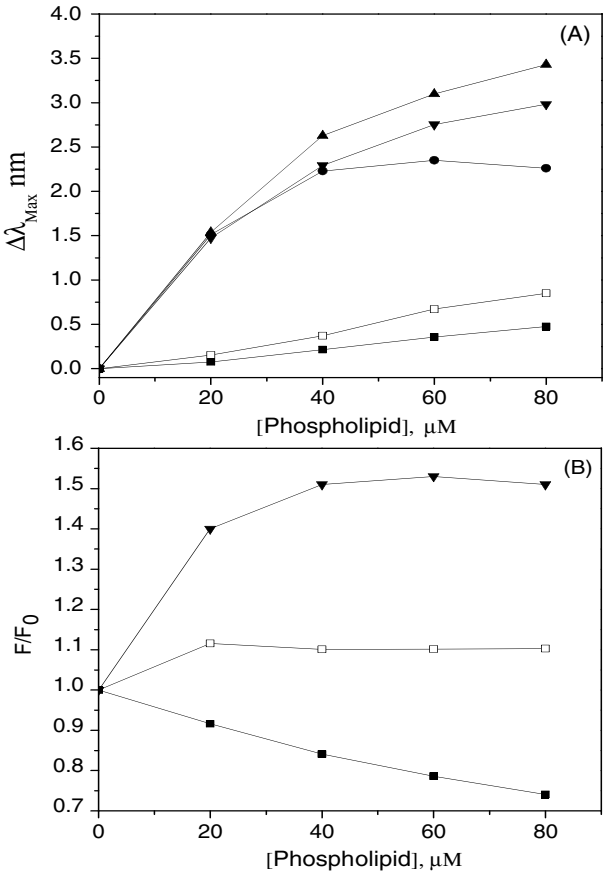

Fig. 9 *Panel A*: Blue shift in Texas Red emission maximum in the presence of liposomes composed of SOPC with X_{POPG} = 0 (□), 0.1 (●), 0.2 (▲), 0.4 (▼), and X_{Chol} = 0.1 (■) as a function of [Phospholipid]. *Panel B*: Changes in fluorescence intensity as a function of phospholipid concentration for SOPC with X_{POPG} = 0 (□), 0.4 (▼), and X_{Chol} = 0.1 (■)

Texas Red moiety. The blue shifts of the emission maxima in the presence of SOPC and SOPC/POPG vesicles reveal that TR inserts into the bilayer. Compared with the zwitterionic membranes, larger values of $\Delta\lambda_{max}$ in TRC-temB emission and diminished quenching by FCN were evident for membranes containing the negatively charged POPG. These differences could be due to a larger fraction of the added peptide being inserted, deeper penetration into the bilayer, or both. While having a random structure in solution C-temB becomes more α-helical in the presence of membranes containing POPG, compared to SOPC (Fig. 2). Accordingly, it could not be ruled out that some of the fluorescence changes seen here result from conformational changes in TRC-temB following its association with liposomes and do not reflect direct changes due to embedding the fluorophore in a lipid environment. Both steady state (Fig. 6) and time resolved fluorescence (Fig. 7B) quenching by FCN reveals that the peptide coupled TR is shielded in the presence of liposomes. Moreover, partition coefficients estimated from the binding isotherms of TRC-temB were higher for acidic vesicles (SOPC/POPG) than those with the zwitterionic SOPC (data not shown).

The steady state anisotropy corresponding to the rotational diffusion of the dye is usually very low due to the rapid rotational diffusion of small molecular weight fluorophores [50]. Compared with the zwitterionic membranes, anisotropy values for TRC-temB were higher in the presence of membranes containing the negatively charged POPG, indicating its rotation to become slower and thus revealing augmented interactions between the TRC-temB and the negatively charged membranes as compared to the zwitterionic bilayers (Fig. 4). As this peptide has a net positive charge, electrostatic interactions between TRC-temB and negatively charged membranes are expected, in keeping with the partial reversal of λ_{max} in the presence of salt (Fig. 8). Electrostatic interactions will concentrate the peptide to the negatively charged membranes as indicated also by our RET experiments, which show a similar pattern, with a significant decrease in the fluorescence of NBD due to energy transfer to TRC-temB in the presence of liposomes. RET is much more efficient in the presence of SOPC/POPG (8:2 molar ratios) as compared to neat SOPC liposomes (Fig. 5B). Partial reversal of NBD fluorescence upon the addition of NaCl again emphasizes the role for electrostatics in the interaction of TRC-temB with membranes. Cholesterol attenuates the binding of TRC-temB to the membranes as revealed by steady state anisotropy, resonance energy transfer, and emission maxima measurements. Cholesterol increases acyl chain order [51] and stabilizes the bilayer structure [52], which could prevent the penetration of TRC-temB into the lipid bilayer and decrease the extent of membrane perturbation by this peptide.

Time resolved fluorescence studies provide further insight into the changes in the conformational dynamics of TRC-temB. The value for τ of the fluorophore relates to its microenvironment and reduced polarity of the medium is associated with longer lifetimes [50, 53] as well as an increase in the quantum yield. Compared to the free fluorophore in an aqueous solution TR shows slightly increased value of τ when coupled to peptide. C-temB is amphiphilic in nature and its coupling with TRM could increase the hydrophobicity of the environment of the fluorophore, prolonging τ. The values for τ further increase in the presence of liposomes in keeping with the TR residue residing in a hydrophobic region of the bilayer, as is evident also from the increase in the quantum yield (Fig. 8). These results do confirm that the interaction between TRC-temB and lipid membranes is driven both by electrostatics as well as hydrophobicity.

The interaction between TRC-temB and negatively charged biomembranes seems to provide a suitable environment for the formation of amyloid like fibers (Fig. 3) and we have suggested this property to relate to the cytotoxic activity of antimicrobial and cytotoxic peptides [12, 27, 35]. These results indicate that membrane penetration as well as cooperative interactions accompany the bilayer association of this peptide derivative. The physicochemical basis of amyloid formation remains poorly understood (54–56). There seems to be a consensus about the fact that peptide aggregation being prompted by partial unfolding of proteins [57]. This can be consistently enhanced in a slightly hydrophobic environment at acidic pH [58] and both hydrophobicity and the net charge of the protein seem to be crucial, neutralization of the charges triggering aggregation [59]. Importantly, the physiological relevance of the low dielectricity, acidic milieu in accelerating the formation of amyloid fibrils *in vitro* has been questioned and may as such be effective *in vivo* when the proteins/peptides reside in the lysosomes [35 and references therein].

We may conclude that TRC-temB shows all the characteristic changes for AMPs induced by lipid membranes, should be a useful model peptide. We are currently exploring its antimicrobial activity and interactions with target and non-target biomembranes.

Acknowledgement We are grateful to Dr. Ove Eriksson for his help with the purification and mass spectrometry of the peptides. RS thanks Drs Arimatti Jutila and Juha Matti Alakoskela for their guidance with the instruments used in this study. The authors thank Kristiina Soderholm and Kaija Niva for technical assistance. HBBG is supported by the Finnish Academy and Sigrid Juselius Foundation.

References

1. Yeaman MR, Yount NY (2003) Mechanisms of antimicrobial peptide action and resistance. Pharmacol Rev 55:27–55
2. Brown KL, Hancock RE (2006) Cationic host defense (antimicrobial) peptides. Curr Opin Immunol 18:24–30

3. Van't Hof W, Veerman EC, Helmerhorst EJ, Amerongen AV (2001) Antimicrobial peptides: properties and applicability. Biol Chem 382:597–619
4. Gennis RP (1989) Biomembranes: molecular structure and function. Springer-Verlag, New York
5. Sitaram N, Nagaraj R (1999) Interaction of antimicrobial peptides with biological and model membranes: structural and charge requirements for activity. Biochim Biophys Acta 1462:29–54
6. Zhao H, Mattila JP, Holopainen JM, Kinnunen PKJ (2001) Comparison of the membrane association of two antimicrobial peptides, magainin 2 and indolicidin. Biophys J 81:2979–2991
7. Zhang L, Scott MG, Yan H, Meyer LD, Hancock REW (2000) Interaction of polyphemusin I and structural analogs with bacterial membranes, lipopolysaccharide, and lipid monolayers. Biochemistry 39:14504–14514
8. Matsuzaki K, Harada M, Funakoshi S, Fujii N, Miyajima K (1991) Physicochemical determinants for the interactions of magainins 1 and 2 with acidic lipid bilayers. Biochim Biophys Acta 1063:162–170
9. Gomes AV, Waal AD, Berden JA, Weaterhoff HV (1993) Electric potentiation, cooperativity, and synergism of magainin peptides in protein-free liposomes. Biochemistry 32:5365–5372
10. Matsuzaki K, Sugishita K, Fujii N, Miyajima K (1995a) Molecular basis for membrane selectivity of an antimicrobial peptide, magainin 2. Biochemistry 34:3423–3429
11. Nelson DL, Cox MM (2000) Lehninger principles of biochemistry. Worth Publishers, New York
12. Zhao H, Jutila A, Nurminen T, Wickstrom SA, Keski-Oja J, Kinnunen PKJ (2005) Binding of endostatin to phosphatidylserine-containing membranes and formation of amyloid like fibers. Biochemistry 44:2857–2863
13. De Kruijff B (1994) Anionic phospholipids and protein translocation. FEBS Lett 346:78–82
14. Kinnunen PKJ, Mouritsen O (1994) Functional dynamics of lipids in biomembranes. Chem Phys Lipids 73:1–2
15. Zhao H, Rinaldi AC, Giulio AD, Simmaco M, Kinnunen PKJ (2002) Interactions of the antimicrobial peptides temporins with model biomembranes, comparison of temporins B and L. Biochemistry 41:4425–4436
16. Shin SY, Kang SW, Lee DG, Eom SH, Song WK, Kim JI (2000) CRAMP analogues having potent antibiotic activity against bacterial, fungal, and tumor cells without hemolytic activity. Biochem Biophys Res Commun 275:904–909
17. Lee DG, Kim HN, Park Y, Kim HK, Choi BH, Choi CH, Hahm KS (2002) Design of novel analogue peptides with potent antibiotic activity based on the antimicrobial peptide, HP (2–20), derived from *N*-terminus of Helicobacter pylori ribosomal protein L1. Biochim Biophys Acta 1598:185–194
18. Lee DG, Kim PI, Park Y, Woo ER, Choi JS, Choi CH, Hahm KS (2002) Design of novel peptide analogs with potent fungicidal activity based on PMAP-23 antimicrobial peptide isolated from porcine myeloid. Biochem Biophys Res Commun 293:231–238
19. Avrahami D, Shai Y (2002) Conjugation of a magainin analogue with lipophilic acids controls hydrophobicity, solution assembly, and cell selectivity. Biochemistry 41:2254–2263
20. Lee KH, Oh JE (2000) Design and synthesis of novel antimicrobial pseudopeptides with selective membrane-perturbation activity. Bioorg Med Chem 8:833–839
21. Oh D, Shin SY, Lee S, Kang JH, Kim SD, Ryu PD, Hahm KS, Kim Y (2000) Role of the hinge region and the tryptophan residue in the synthetic antimicrobial peptides, cecropin A(1–8)-magainin 2(1–12) and its analogues, on their antibiotic activities and structures. Biochemistry 39:11855–11864
22. Travis SM, Anderson NN, Forsyth WR, Espiritu C, Conway BD, Greenberg EP, McCray PB, Lehrer RI, Welsh MJ, Track BF (2000) Bactericidal activity of mammalian cathelicidin-derived peptides. Infect Immun 68:2748–2755
23. Bucki R, Pastore JJ, Randhawa P, Vegners R, Weiner DJ, Janmey PA (2004) Antibacterial activities of rhodamine B-conjugated gelsolin-derived peptides compared to those of the antimicrobial peptides cathelicidin LL37, magainin II, and melittin. Antimicrobial Agents and Chemotherapy 48:1526–1533
24. Zhao H, Kinnunen PKJ (2002) Binding of the antimicrobial peptide temporin L to liposomes assessed by Trp fluorescence. J Biol Chem 277:25170–25177
25. Pouny Y, Rapaport D, Mor A, Nicolas P, Shai Y (1992) Interaction of antimicrobial dermaseptin and its fluorescently labeled analogs with phospholipid membranes. Biochemistry 31:12416–12423
26. Gazit E, Boman A, Boman HG, Shai Y (1995) Interaction of the mammalian antibacterial peptide cecropin P1 with phospholipid vesicles. Biochemistry 34:11479–11488
27. Zhao H, Sood R, Jutila A, Bose S, Fimland G, Meyer JN, Kinnunen PKJ (2006) Interaction of the antimicrobial peptide pheromone Plantaricin A with model membranes: implications for a novel mechanism of action. Biochim Biophys Acta 1758:1461–74
28. Bechinger B (1997) Structure and functions of channel-forming peptides: magainin, cecropins, mellitin and alamethicin. J Membr Biol 156:197–211
29. Matsuzaki K (1998) Magainins as paradigm for the mode of action of pore forming polypeptides. Biochim Biophys Acta 1376:391–400
30. Matsuzaki K (1999) Why and how are peptide-lipid interactions utilized for self-defense? Magainins and tachyplesins as archetypes. Biochim Biophys Acta 1462:1–10
31. Oren Z, Shai Y (1998) Mode of action of linear amphipathic α-helical antimicrobial peptides. Biopolymers (Peptide Sci) 47:451–463.
32. Shai Y (1999) Mechanism of the binding, insertion, and destabilization of phospholipid bilayer membranes by α-helical antimicrobial and cell non-selective membrane-lytic peptides. Biochim Biophys Acta 1462:55–70
33. Dobson CM (2003) Protein folding and misfolding. Nature 426:884–890
34. Uversky VN, Fink AL (2004) Conformational constraints for amyloid fibrillation: the importance of being unfolded. Biochim Biophys Acta 1698:131–153
35. Zhao H, Tuominen EKJ, Kinnunen PKJ (2004) Formation of amyloid fibers triggered by phosphatidylserine-containing membranes. Biochemistry 43:10302–10307
36. Gorbenko GP, Kinnunen PKJ (2006) The role of lipid-protein interactions in amyloid-type protein fibril formation. Chem Phys Lipids 141:72–82
37. Simmaco M, Mignogna G, Canofeni S, Miele R, Mangoni ML, Barra D (1996) Temporins, novel antimicrobial peptides from the European red frog *Rana temporaria*. Eur J Biochem 242:788–792
38. Goraya J, Wang Y, Li Z (2000) Peptides with antimicrobial activity from four different families isolated from the skins of the North American frogs *Rana luteiventris*, *Rana berlandieri*, and *Rana pipiens*. Eur J Biochem 276:894–900
39. Halverson T, Basir YJ, Knoop FC, Conlon JM (2000) Purification and characterization of antimicrobial peptides from the skin of the North American green frog *Rana clamitans*. Peptides 21:469–476
40. Kim JB, Halverson T, Basir YJ, Dulka J, Knoop FC, Abel PW, Conlon JM (2000) Purification and characterization of antimicrobial and vasorelaxant peptides from skin extracts and skin secretions of the North American pig frog *Rana grylio*. Regul Pept 90:53–60
41. Harjunpaa I, Kuusela P, Smoluch MT, Silberring J, Lankinen H, Wade D (1999) Comparison of synthesis and antibacterial activity of temporin A. FEBS Lett 449:187–190.

42. Mangoni ML, Rinaldi AC, Giulio AD (2000) Structure-function relatioships of temporins, small antimicrobial peptides from amphibian skin. Eur J Biochem 267:1447–1454
43. Wiedmer SK, Hautala J, Holopainen JM, Kinnunen PKJ, Riekkola ML (2001) Study on liposomes by capillary electrophoresis. Electrophoresis 22:1305–1313
44. Bernstein LS, Grillo AA, Loranger SS, Linder ME (2000) RGS4 binds to membranes through an amphipathic α-Helix. J Biol Chem 275:18520–18526
45. Torimura M, Kurata S, Yamada K, Yokomaku T, Kamagata Y, Kanagawa T, Kurane R (2001) Fluorescence quenching phenomenon by photoinduced electron transfer between a fluorescent dye and a nucleotide base. Anal Sci 17:155–160
46. Bevington PR (1969) Data reduction and error analysis for the physical sciences. McGraw-Hill, New York
47. Lampert RA, Chewter LA, Phillips D, O'Connor DV, Roberts AJ, Meech SR (1983) Standards for nanosecond fluorescence decay time measurements. Anal Chem 55:68–73
48. Grinvald A, Steinberg IZ (1974) On the analysis of fluorescence decay kinetics by the method of least-squares. Anal Biochem 59:583–598
49. McElhaney RN, Prenner EJ (eds) (1999) Special Issue on Antimicrobial Peptides. Biochim Biophys Acta 1462:1–234
50. Lakowicz JR (1999) Principles of fluorescence spectroscopy. Kluwer Academic/Plenum Publishers, New York
51. Yeagle PL (1985) Lanosterol and cholesterol have different effects on phospholipid acyl chain ordering. Biochim Biophys Acta 815:33–36
52. Cullis PR, Dijck PWM, de Kruijff B, de Gier J (1978) Effects of cholesterol on the properties of equimolar mixtures of synthetic phosphatidylethanolamine and phosphatidylcholine, A ^{31}P NMR and differential scanning calorimetry study. Biochim Biophys Acta 513:21–30
53. Wiczk W, Mrozek J, Szabelski M, Karolczak J, Guzow K, Malicka J (2001) Determination of stoichiometry and equilibrium constants of complexes of tyrosine with cyclodextrins by time resolved fluorescence spectroscopy and global analysis of fluorescence decays. Chem Phys Lett 341:161–167
54. Aguzzi A, Haass C (2003) Games played by rogue proteins in prion disorders and Alzheimer's disease. Science 302:814–818
55. Kayed R, Head E, Thompson JL, McIntire TM, Milton SC, Cotman CW, Glabe CG (2003) Common structure of soluble amyloid oligomers implies common mechanism of pathogenesis. Science 300:486–489
56. Rochet JC, Lansbury Jr PT (2000) Amyloid fibrillogenesis: themes and variations. Curr Opin Struct Biol 10:60–68
57. Kinnunen PKJ, Koiv A, Lehtonen JY, Rytömaa M, Mustonen P (1994) Lipid dynamics and peripheral interactions of proteins with membrane surfaces. Chem Phys Lipids 73:181–207
58. Whittingham JL, Scott DJ, Chance K, Wilson A, Finch J, Brange J, Dodson GG (2002) Insulin at pH 2: structural analysis of the conditions promoting insulin fibre formation. J Mol Biol 318:479–490
59. Bokvist M, Lindstrom F, Watts A, Grobner G (2004) Two types of Alzheimer's β-amyloid (1–40) peptide membrane interactions: aggregation preventing transmembrane anchoring versus accelerated surface fibril formation. J Mol Biol 335:1039–1049